

Overexpression of a Novel Class of Gibberellin 2-Oxidases Decreases Gibberellin Levels and Creates Dwarf Plants

Fritz M. Schomburg,^{a,1} Colleen M. Bizzell,^{a,1} Dong Ju Lee,^b Jan A. D. Zeevaart,^{b,c,2} and Richard M. Amasino^{a,2}

^a Department of Biochemistry, University of Wisconsin–Madison, Madison, Wisconsin 53706

^b Department of Energy Plant Research Laboratory, Michigan State University, East Lansing, Michigan 48824-1312

^c Department of Plant Biology, Michigan State University, East Lansing, Michigan 48824-1312

Degradation of active C₁₉-gibberellins (GAs) by dioxygenases through 2 β -hydroxylation yields inactive GA products. We identified two genes in Arabidopsis (*AtGA2ox7* and *AtGA2ox8*), using an activation-tagging mutant screen, that encode 2 β -hydroxylases. GA levels in both activation-tagged lines were reduced significantly, and the lines displayed dwarf phenotypes typical of mutants with a GA deficiency. Increased expression of either *AtGA2ox7* or *AtGA2ox8* also caused a dwarf phenotype in tobacco, indicating that the substrates for these enzymes are conserved. *AtGA2ox7* and *AtGA2ox8* are more similar to each other than to other proteins encoded in the Arabidopsis genome, indicating that they may constitute a separate class of GA-modifying enzymes. Indeed, enzymatic assays demonstrated that *AtGA2ox7* and *AtGA2ox8* both perform the same GA modification: 2 β -hydroxylation of C₂₀-GAs but not of C₁₉-GAs. Lines containing increased expression of *AtGA2ox8* exhibited a GA dose–response curve for stem elongation similar to that of the biosynthetic mutant *ga1-11*. Double loss-of-function *Atga2ox7 Atga2ox8* mutants had twofold to fourfold higher levels of active GAs and displayed phenotypes associated with excess GAs, such as early bolting in short days, resistance to the GA biosynthesis inhibitor ancymidol, and decreased mRNA levels of *AtGA20ox1*, a gene in the GA biosynthetic pathway.

INTRODUCTION

The gibberellins (GAs) are a class of plant hormones that are involved in a variety of growth and developmental processes, including seed germination, leaf expansion, stem elongation, floral induction, fruit maturation, and apical dominance (Harberd et al., 1998). GAs are substituted tetracyclic diterpene carboxylic acids that require many biosynthetic steps to create (for review, see Hedden and Phillips, 2000). To date, 126 different GAs have been identified in plants, fungi, and bacteria (<http://www.plant-hormones.info/gibberellins.htm>); however, most of these are precursors or degradation products. Examples of bioactive GAs synthesized by higher plants are GA₁, GA₃, GA₄, and GA₇ (Hedden and Phillips, 2000).

The GA biosynthetic pathway can be classified into three stages (Olszewski et al., 2002). In the first stage, geranylgeranyl diphosphate is cyclized to *ent*-kaurene by copalyl diphosphate synthase and *ent*-kaurene synthase. In the second stage, *ent*-kaurene is oxidized by *ent*-kaurene oxidase to *ent*-kaurenoic acid, which in turn is oxidized by *ent*-kaurenoic acid oxidase in three steps to GA₁₂. All reactions in

stage 2 are catalyzed by cytochrome P450 monooxygenases (Helliwell et al., 1998, 2001). In the third stage, GA₁₂ is modified by oxidative reactions involving 2-oxoglutarate-dependent dioxygenases. In the first reaction of the third stage, C-20 is oxidized and removed. In Arabidopsis, this is followed by 3 β -hydroxylation to give bioactive GA₁ and GA₄ (Hedden and Phillips, 2000).

Mutants in GA biosynthesis have been identified in a variety of species. In Arabidopsis, the most prominent phenotypes of GA biosynthesis mutants are reduced internode length and small dark green leaves (Koorneef and van der Veen, 1980). In such mutants, normal growth can be restored by the application of active GAs. The *ga1-3* mutation is thought to represent the most complete block to GA biosynthesis because *ga1-3* mutants display the most severe GA-deficient phenotypes (Wilson et al., 1992) and the *GA1* gene encodes the only copy of copalyl diphosphate synthase in Arabidopsis (Sun and Kamiya, 1994). Mutations in genes involved in the later stages of GA biosynthesis in Arabidopsis, such as *ga4* and *ga5*, cause a less severe or semi-dwarf phenotype (Talon et al., 1990a). GA5 enzymatic activity is encoded by a small gene family of GA 20-oxidases (Phillips et al., 1995). Thus, functional redundancy is likely to be the reason that mutations in genes involved in the later stages of GA biosynthesis result in a phenotype that is less severe than that of *ga1*.

¹ These authors contributed equally to this work.

² To whom correspondence should be addressed. E-mail amasino@biochem.wisc.edu; fax 608-262-3453.

Article, publication date, and citation information can be found at www.plantcell.org/cgi/doi/10.1105/tpc.005975.

In contrast to biosynthesis, less is known about the pathways and regulation of GA degradation. The first step in the degradation of biologically active GAs involves reactions similar to those seen in the final steps of GA biosynthesis. For example, the last step of GA biosynthesis involves a 3 β -hydroxylase (also referred to as 3-oxidase) that introduces a hydroxyl group at the C-3 of GA precursors to form active GAs (Talon and Zeevaert, 1992; Chiang et al., 1995). The first step of GA degradation involves GA 2-oxidases that hydroxylate the C-2 of active GAs (Martin et al., 1999; Thomas et al., 1999; Sakamoto et al., 2001). Thus, the site of similar hydroxylation reactions determines the activity of GA molecules.

GA 2-oxidase genes have been cloned from several species, including three from *Arabidopsis* (Thomas et al., 1999). These GA 2-oxidases use C₁₉-GAs as their substrates. Expression studies of the three *Arabidopsis* 2-oxidases revealed that two of them were most abundant in the inflorescence and developing siliques, whereas the other one could not be detected in any tissue (Thomas et al., 1999). This expression pattern is consistent with a role of GA 2-oxidases in reducing GA levels in seeds to promote dormancy. Further evidence for this role comes from studies of the *SLENDER* gene of pea, which also encodes a GA 2-oxidase (Martin et al., 1999). The hyperelongation of the *slender* mutant phenotype is most apparent in seedlings. This mutation results in high levels of GA precursors in seeds, which are converted to active GAs upon germination. This excess GA causes the *slender* seedling phenotype (Martin et al., 1999).

Here, we describe the identification of novel GA 2-oxidases in *Arabidopsis* that hydroxylate C₂₀-GA precursors but not C₁₉-GAs. We demonstrate that increased expression of these 2-oxidases results in decreased levels of active GAs and corresponding dwarf phenotypes in *Arabidopsis* and tobacco. Loss of these oxidases in *Arabidopsis* results in increased levels of active GAs and in phenotypes associated with increased GA levels.

RESULTS

Activation Tagging of Loci That Confer a Dominant Dwarf Phenotype

A mutant screen was performed using T-DNA from the pSKI015 activation-tagging vector as the mutagen. This vector contains four repeats of the enhancer region of the constitutively expressed 35S promoter of *Cauliflower mosaic virus* (CaMV) in the T-DNA, and introduction of this T-DNA into the genome can cause increased gene expression near the site of integration in an orientation-independent manner (Weigel et al., 2000). Dominant phenotypes are observed in the first mutagenized (T1) generation. In this screen, we identified two dwarf mutants (Figure 1A) from ~60,000 independent T1 lines of *Arabidopsis* (accession Wassilewskija) grown in long-day photoperiods.

Both mutant phenotypes appeared to be caused by T-DNA insertion, because in the subsequent (T2) generation, the T-DNA was present in all mutant plants and wild-type plants lacked the T-DNA. In both mutants, the dwarf trait was dominant: the T2 generation segregated 3:1 (dwarf to wild-type plants). The dominance of the dwarf trait indicated that the mutations likely resulted from increased gene expression from the 35S enhancers in the T-DNA.

Identification of the Dominant Dwarfing Genes

To identify the genes responsible for the mutant phenotypes, the sites of the T-DNA insertions were characterized. The junction between the T-DNA and *Arabidopsis* genomic DNA was determined by thermal asymmetrical interlaced (TAIL)-PCR (see Methods). In both mutants, the T-DNA insertion of the right border (which contains the 35S enhancer regions) was positioned at the 5' end of the predicted genes, as illustrated in Figure 2. The mutant lines are referred to here as *AtGA2ox7_{ACT}* and *AtGA2ox8_{ACT}*, and the genes predicted to be activated by the T-DNA are designated *AtGA2ox7* and *AtGA2ox8*. The designations *AtGA2ox7* and *AtGA2ox8* were chosen because *AtGA2ox1* through *AtGA2ox3* were described by Thomas et al. (1999) and genes designated *AtGA2ox4* through *AtGA2ox6* were noted by Hedden and Phillips (2000). The genes identified in this study (*AtGA2ox7* and *AtGA2ox8*) are distinct from *AtGA2ox1* through *AtGA2ox6* (P. Hedden and A.L. Phillips, personal communication).

Reverse transcription-based PCR (RT-PCR) showed that the mRNA levels of *AtGA2ox7* and *AtGA2ox8* were increased substantially in the respective mutant lines (Figure 3). To verify that the increased expression of these genes was capable of causing a dwarf phenotype, we attempted to independently recreate the phenotype with constructs designed to increase the expression of these genes. Accordingly, constructs in which the constitutively expressed CaMV 35S promoter was joined to genomic clones of *AtGA2ox7* and *AtGA2ox8* (Figure 2) were introduced into wild-type *Arabidopsis*. The introduction of these constructs was able to recapitulate the dwarf phenotype (Figure 1B, Table 1), confirming the identity of the genes responsible for the dwarf phenotypes.

We determined the cDNA sequences of both genes by RT-PCR and created constructs in which the cDNAs were driven by the CaMV 35S promoter (Figure 2). Increased expression of either cDNA was sufficient to produce dwarf plants (data not shown), demonstrating that biologically active cDNAs for both genes had been identified. The protein sequences predicted by these cDNAs are shown in Figure 4.

The Activation-Tagged Genes Display Similarity to Gibberellin Dioxygenases

Alignments of the *AtGA2ox7* and *AtGA2ox8* predicted proteins indicate that they share similarity to the dioxygenase

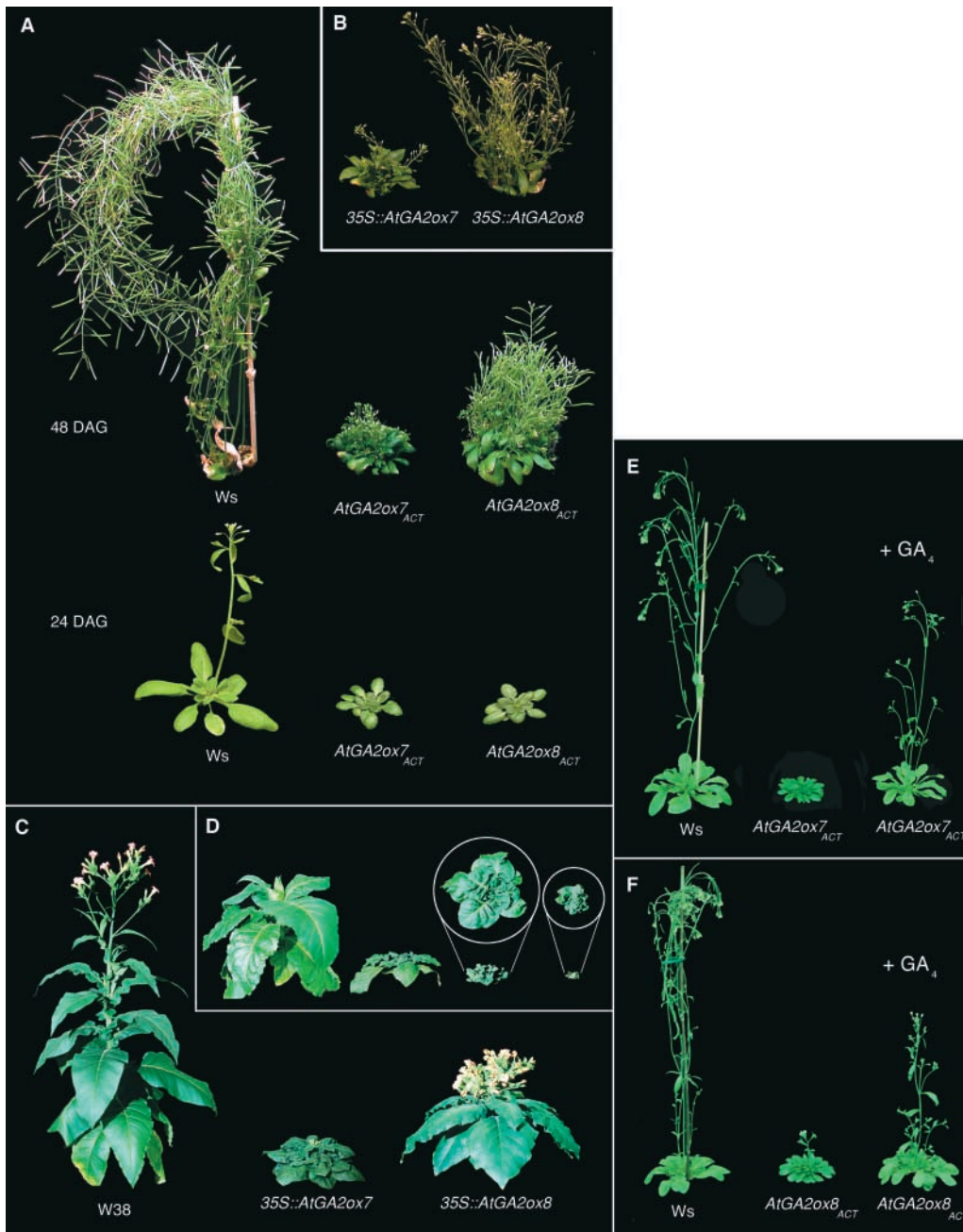


Figure 1. Phenotypes of Arabidopsis (Accession Wassilewskija) and Tobacco (var Wisconsin 38) with Increased Expression Levels of *AtGA2ox7* and *AtGA2ox8*.

- (A) *AtGA2ox7_{ACT}* and *AtGA2ox8_{ACT}* activation-tagged dwarf mutants are shown at 24 and 48 days after germination (DAG). Ws, Wassilewskija.
 (B) Arabidopsis containing the *35S::AtGA2ox7* or *35S::AtGA2ox8* genomic construct.
 (C) Tobacco containing the *35S::AtGA2ox7* or *35S::AtGA2ox8* cDNA construct. W38, Wisconsin 38.
 (D) The range of dwarf phenotypes obtained in transgenic lines containing *35S::AtGA2ox7*.
 (E) and (F) Responses of *AtGA2ox7_{ACT}* and *AtGA2ox8_{ACT}* mutants to GA_4 at 12 and 14 days, respectively, after GA_4 application. Plants were transferred from short days to long days at the start of GA_4 treatment.

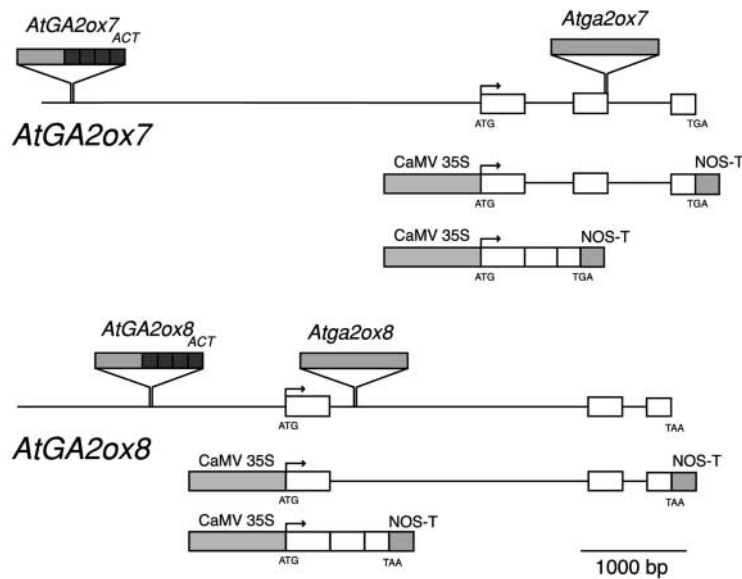


Figure 2. Genomic Structures of *AtGA2ox7* and *AtGA2ox8*.

Boxes represent exons, and the intervening lines denote introns. The locations of T-DNA insertion alleles of *AtGA2ox7* and *AtGA2ox8* are shown as boxes above the genomic structures. T-DNA inserts with dark gray boxes (35S enhancers) denote the activation-tagged alleles, whereas the monochromatic gray T-DNA inserts denote knockout allele insertions. Overexpression constructs for genomic and cDNA clones are shown below the genomic regions of *AtGA2ox7* and *AtGA2ox8*, respectively. NOS, nopaline synthase.

family of GA-modifying enzymes (Table 2). *AtGA2ox7* and *AtGA2ox8* are more similar to each other than to any other predicted protein in the Arabidopsis genome, indicating that these genes may constitute a separate branch of GA metabolism (Table 2, Figure 4). The closest match in the Arabidopsis genome is *AtGA2ox1*, which is 32% identical to both *AtGA2ox7* and *AtGA2ox8*. The overall relatedness of the GA-modifying dioxygenase enzymes is not surprising, because these enzymes are likely to have conserved motifs that bind GAs and other common cofactors. However, a unique region of similarity between *AtGA2ox7* and *AtGA2ox8* (at positions 115 to 143 of *AtGA2ox8*; Figure 4) may define the specificity of the reactions performed by these enzymes.

Overexpression of *AtGA2ox7* and *AtGA2ox8* in Tobacco Results in Dwarf Phenotypes

To determine whether the overexpression of *AtGA2ox7* or *AtGA2ox8* would cause a GA-deficient phenotype in a different plant species, the 35S promoter–*AtGA2ox7* and –*AtGA2ox8* cDNA fusion constructs were transformed into the Wisconsin 38 variety of tobacco. Overexpression of both *AtGA2ox7* and *AtGA2ox8* caused dwarfing (Figures 1C and 1D), indicating that the substrates for these enzymes are required for normal elongation growth in tobacco. A range of dwarf phenotypes was observed with the overex-

pression of both genes; however, *AtGA2ox7* overexpression generally caused a more severe dwarf phenotype than did *AtGA2ox8* overexpression (similar to the effects of overexpression in Arabidopsis). Transgenic lines were obtained with phenotypes that ranged from nearly wild type to severely dwarf compact rosettes that had no discernible internodes (Figures 1C and 1D). This is likely the result of copy number and/or transgene position effect variation in expression. Because the expression of *AtGA2ox7* and *AtGA2ox8* can generate plants that display a range of dwarf phenotypes in Arabidopsis and tobacco, which are species in the two major clades of eudicots (Soltis et al., 1999), these genes may prove broadly useful in agriculture to control plant stature without the use of chemical treatments to inhibit GA biosynthesis.

AtGA2ox7 and *AtGA2ox8* Proteins Render C_{20} -GA Precursors Inactive by Hydroxylation of the 2 Position

To investigate the reactions catalyzed by *AtGA2ox7* and *AtGA2ox8*, we produced the proteins in *Escherichia coli* for enzyme assays. Specifically, the cDNAs were cloned into the pET-28a vector, which permits inducible protein production in *E. coli*, and total cellular lysates of induced cells were used for enzyme assays. Substrate and product(s) were separated by reverse-phase HPLC with online radioactivity

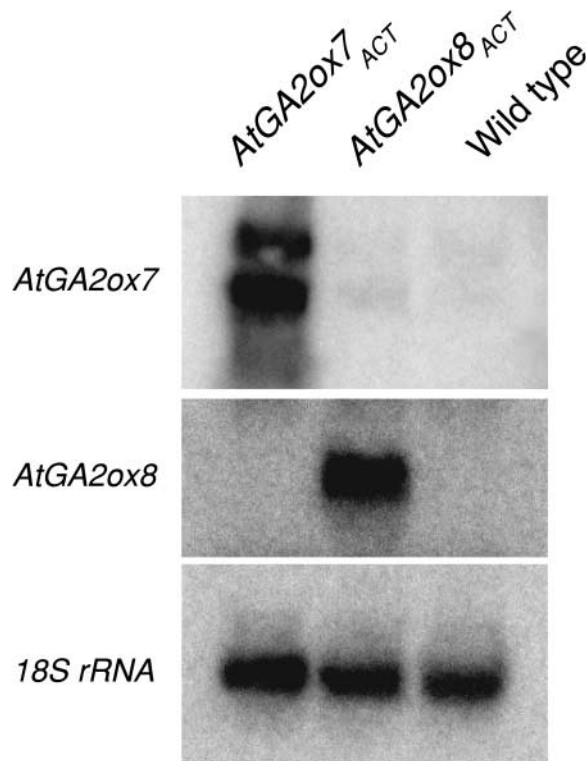


Figure 3. Expression Analysis of Activation-Tagged Alleles of *AtGA2ox7* and *AtGA2ox8*.

Twenty-two cycles of RT-PCR were used to amplify *AtGA2ox7* and *AtGA2ox8*. Fourteen cycles of RT-PCR were used to amplify 18S rRNA.

detection. The results for *AtGA2ox7* are presented in Table 3; similar results were obtained for *AtGA2ox8* (data not shown). When ^{14}C - GA_{12} (retention time = 35.7 min) was used as a substrate, a product with a retention time of 26.6 min was formed with both enzymes. This product was iden-

tified by gas chromatography–mass spectrometry as ^{14}C - GA_{110} . In the case of ^{14}C - GA_{53} (retention time = 29.7 min) as a substrate, the product was identified as ^{14}C - GA_{97} (retention time = 12.6 min). Thus, both proteins are able to catalyze the 2 β -hydroxylation of the C_{20} -GA precursors GA_{12} and GA_{53} . By contrast, the C_{19} -GAs, GA_1 , GA_4 , GA_9 , and GA_{20} , with a γ -lactone ring were not 2 β -hydroxylated by these enzymes. Thus, *AtGA2ox7* and *AtGA2ox8* represent a new class of 2-oxidases that specifically inactivate C_{20} -GA precursors. All previously characterized GA 2-oxidases 2 β -hydroxylate predominantly C_{19} -GAs (Martin et al., 1999; Thomas et al., 1999; Sakamoto et al., 2001). Several putative GAs have been detected in extracts of *Arabidopsis* (Talon et al., 1990b). Two of these compounds have been identified as GA_{97} and GA_{110} (J.A.D. Zeevaart, unpublished results), indicating that *AtGA2ox7* and *AtGA2ox8* do function in vivo.

Increased Expression of *AtGA2ox7* or *AtGA2ox8* Affects GA Levels but Not GA Responsiveness

The levels of endogenous GAs were much reduced in the *AtGA2ox7*_{ACT} and *AtGA2ox8*_{ACT} plants compared with those in wild-type plants (Table 4). The level of bioactive GA_4 was below the limit of detection in both mutants. Thus, the dwarf phenotype is attributable to GA deficiency. This result is further supported by the observation that the application of GA restores normal stem growth and flowering time in *AtGA2ox7*_{ACT} and *AtGA2ox8*_{ACT} plants (Figures 1E and 1F), and a comparison of *AtGA2ox8*_{ACT} with the biosynthetic mutant *ga1-11* revealed the same dose–response relationship for stem elongation in both lines (Figure 5).

Altered Expression of *AtGA2ox7* and *AtGA2ox8* Affects Flowering Behavior

Decreased GA levels severely delay floral induction in *Arabidopsis* in noninductive short days and also cause a slight

Table 1. Phenotypic Characterization of the Overexpression Lines of *AtGA2ox7* and *AtGA2ox8*

Trait	Wild Type	<i>AtGA2ox7</i> _{ACT}	<i>AtGA2ox8</i> _{ACT}	35S:: <i>AtGA2ox7</i>	35S:: <i>AtGA2ox8</i>
Flowering behavior ^a (number of leaves)	8.1 (1.0)	15.0 (1.1)	13.8 (1.5)	16.2 (1.6)	14.9 (1.7)
Height (cm)	48 (1.1)	7.5 (1.0)	9.6 (1.3)	8.2 (1.3)	9.6 (1.3)
Number of inflorescence branches ^b	41 (5.3)	87 (28)	84 (25)	>100	>100
Internode length (mm) ^c	9.1 (0.13)	1.9 (0.27)	2.4 (0.37)	2.5 (0.49)	2.7 (0.57)

Plants were grown in long-day photoperiods. Numbers in parentheses indicate 1 SD. Flowering time was scored upon the emergence of floral buds.

^aNumber of rosette leaves formed by the primary meristem before the transition to flowering.

^bTotal number of inflorescences and inflorescence branches produced.

^cInternode length between siliques on the primary inflorescence measured as $(n-1)/L$, where n is the total number of siliques and L is the length of the inflorescence containing siliques.



Figure 4. Alignment of the Sequences of AtGA2ox7 and AtGA2ox8 Predicted Proteins.

Black shading indicates identical amino acid residues, and gray shading indicates similar residues. The region denoted by a bar above the peptide sequences from positions 115 to 143 is unique to these two proteins in Arabidopsis.

delay in inductive long days (Wilson et al., 1992). Because *AtGA2ox7_{ACT}* and *AtGA2ox8_{ACT}* have reduced levels of active GAs, it was not surprising to find that these mutants behaved similarly to known GA-deficient mutants: *AtGA2ox7_{ACT}* and *AtGA2ox8_{ACT}* plants flowered slightly later in long days (producing 15 and 14 leaves on the primary stem versus 8 leaves for the wild type; Table 1) and flowered much later in short days (producing >80 leaves versus an average of 30 leaves for the wild type). The application of GA₃ was sufficient to rescue this late-flowering phenotype (data not shown), indicating that the decreased level of GA was responsible for the delay in flowering.

To determine whether flowering was affected by loss-of-function mutations in *AtGA2ox7* and *AtGA2ox8*, mutant lines that contained T-DNAs inserted in the coding region of *AtGA2ox7* and *AtGA2ox8* were obtained from the Arabidopsis Knockout Facility at the University of Wisconsin (Krysan et al., 1999). The *Atga2ox7* mutant line contained a T-DNA insertion at the 3' end of the second exon, and the *Atga2ox8* mutant line contained a T-DNA insertion at the beginning of the first intron (Figure 2). A double mutant that contained both lesions (*Atga2ox7 Atga2ox8*) was obtained from an F2 population derived from a cross of the two single mutants. The flowering behavior of the loss-of-function mutants was evaluated in long and short days. There were no significant differences in the flowering behavior of the loss-of-function mutants versus the wild type in long days, but in short days, *Atga2ox8* and *Atga2ox7 Atga2ox8* mutants formed fewer rosette leaves before bolting (Figure 6A). However, the number of cauline leaves formed in short days was greater in the *Atga2ox8* and *Atga2ox7 Atga2ox8* lines compared with the wild type. Therefore, the total number of leaves produced on the primary stem was not significantly different from that produced in the wild type (Figure 6A). Rather, the ratio of cauline leaves to rosette leaves increased in both *Atga2ox8*

and *Atga2ox7 Atga2ox8* mutants (Figure 6B), indicating that the reduced rosette leaf number of these lines in short days likely resulted from the relocation of leaves that would have been present in the wild-type rosette to the inflorescence stem.

Loss-of-Function Mutants Display GA Excess Phenotypes

Increased expression of *AtGA2ox7* and *AtGA2ox8* causes a decrease in GA levels; therefore, loss-of-function mutations

Table 2. Comparison of AtGA2ox7 and AtGA2ox8 Proteins with Other Arabidopsis GA Dioxygenases

	2ox7	2ox8	2ox1	2ox2	2ox3	20ox1	20ox2	20ox3	3ox1	3ox2
2ox7	44	27	25	25	32	31	31	28	28	
2ox8		29	26	27	32	30	31	29	25	
2ox1			55	53	31	29	29	31	32	
2ox2				69	28	28	28	34	33	
2ox3					27	30	28	33	32	
20ox1						73	61	31	29	
20ox2							64	32	30	
20ox3								32	32	
3ox1									74	
3ox2										74

Numbers denote percentage identity between predicted proteins. Thick lines separate the functional classes of dioxygenases. 2ox7 and 2ox8 indicate AtGA2ox7 and AtGA2ox8, respectively. 2ox1 through 2ox3 represent the GA 2-oxidases AtGA2ox1 through AtGA2ox3. 20ox1 through 20ox3 represent the GA 20-oxidases AtGA20ox1 through AtGA20ox3. 3ox1 and 3ox2 indicate the GA 3-oxidases AtGA3ox1 and AtGA3ox2.

Table 3. Identification of Products Formed by the Incubation of Recombinant GA 2-Oxidase (AtGA2ox7) with GA₁₂ or GA₅₃

Substrate	Product	Mass Spectra of Products ^a [mass-to-charge ratio (% relative abundance)]
¹⁴ C ₄ -GA ₁₂	¹⁴ C ₄ -GA ₁₁₀	M ⁺ 456 (11), 448 (8), 441 (11), 433 (8), 424 (51), 416 (44), 396 (78), 388 (66), 379 (7), 373 (7), 322 (13), 316 (10), 306 (100), 298 (92), 291 (71), 283 (64), 262 (27), 261 (28), 258 (23), 257 (26), 245 (98), 239 (74), 229 (37), 223 (24), 199 (16), 197 (12), 147 (37), 145 (41)
¹⁴ C ₄ -GA ₅₃	¹⁴ C ₄ -GA ₉₇	M ⁺ 544 (45), 536 (22), 529 (12), 521 (5), 510 (5), 504 (4), 483 (13), 477 (6), 452 (3), 446 (2), 393 (8), 387 (4), 377 (5), 371 (4), 331 (5), 327 (5), 301 (5), 297 (3), 243 (19), 239 (17), 210 (73), 209 (100), 208 (31), 207 (56)

^a As the methyl ester trimethylsilyl ethers.

in these genes might lead to increased GA levels. To test for phenotypic changes consistent with increased GA levels in the *Atga2ox7* and *Atga2ox8* mutants, hypocotyl lengths in several light conditions and the ability of seeds to germinate in the presence of the GA biosynthesis inhibitor ancymidol were evaluated. To control for environmentally caused variability in seed dormancy and seedling traits, seeds were harvested from several wild-type, single mutant, and *Atga2ox7 Atga2ox8* double mutant plants that were derived from a single F2 population grown in the same flat. Seeds from several individual plants of each genotype were used for each assay, and each assay was performed at least twice.

Although germination was inhibited completely at 16 μM ancymidol in all lines, both *Atga2ox8* and *Atga2ox7 Atga2ox8* were more resistant to 4 and 8 μM ancymidol concentrations than were *Atga2ox7* and the wild type (Figure 7). Thus, one role of *AtGA2ox8* may be to inhibit seed germination. The *Atga2ox7 Atga2ox8* double mutant did not display an increased propensity for germination on ancymidol plates compared with *Atga2ox8* mutants, indicating that *AtGA2ox8* and *AtGA2ox7* functions do not overlap in seed dormancy.

Atga2ox8 and *Atga2ox7 Atga2ox8* mutants displayed longer hypocotyls compared with wild-type seedlings in medium-light (50 μmol·m⁻²·s⁻¹; Figure 8) and low-light (15 μmol·m⁻²·s⁻¹; data not shown) conditions. Although the hypocotyl length of *Atga2ox7* mutants was not significantly different from

that of the wild type, the hypocotyls of the *Atga2ox7 Atga2ox8* double mutants were longer than those of the *Atga2ox8* single mutant. Thus, *AtGA2ox7* and *AtGA2ox8* both may function in the control of hypocotyl elongation.

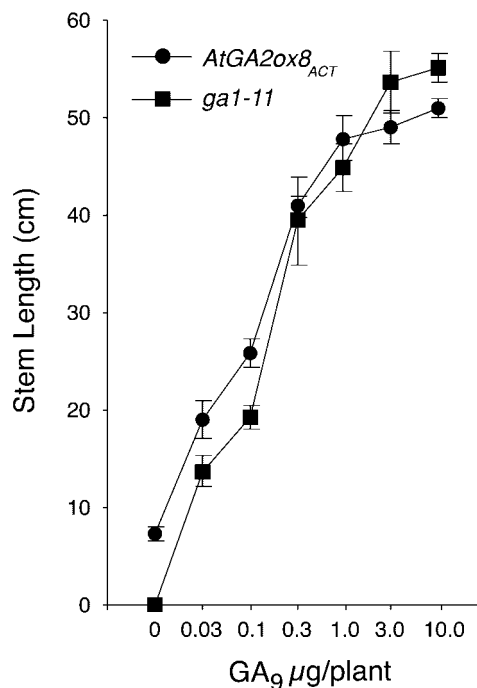
Loss-of-Function Mutants Possess Higher Levels of Active GAs and Decreased GA Biosynthetic Activity

Gas chromatography–selected ion monitoring analyses showed that *Atga2ox7 Atga2ox8* mutants contain increased

Table 4. GA Content of Wild-Type Arabidopsis (Accession Wassilewskija [Ws]) and *AtGA2ox7_{ACT}* and *AtGA2ox8_{ACT}* Lines

GAs	Ws	<i>AtGA2ox7_{ACT}</i>	<i>AtGA2ox8_{ACT}</i>
Non-13-hydroxylated			
GA ₂₄	51.8	0.06	0.23
GA ₉	1.01	0.02	0.05
GA ₄	1.84	ND	ND
13-Hydroxylated			
GA ₅₃	6.43	0.39	0.30
GA ₄₄	0.79	ND	ND
GA ₁₉	9.29	0.02	0.09
GA ₂₀	0.19	ND	ND
GA ₁	0.12	ND	0.02

All values are ng/g dry weight. ND, not detectable.

**Figure 5.** Stem Elongation Dose–Response Curves for the GA Biosynthetic Mutant *ga1-11* and *AtGA2ox8_{ACT}* Lines.

GA₉ was applied twice (at 0 and 5 days) to the shoot apex of flowering plants to achieve the final amount noted on the x axis. Stems were measured at 20 days after the first GA₉ application. Both genotypes flowered at the same time. Error bars indicate ±SD.

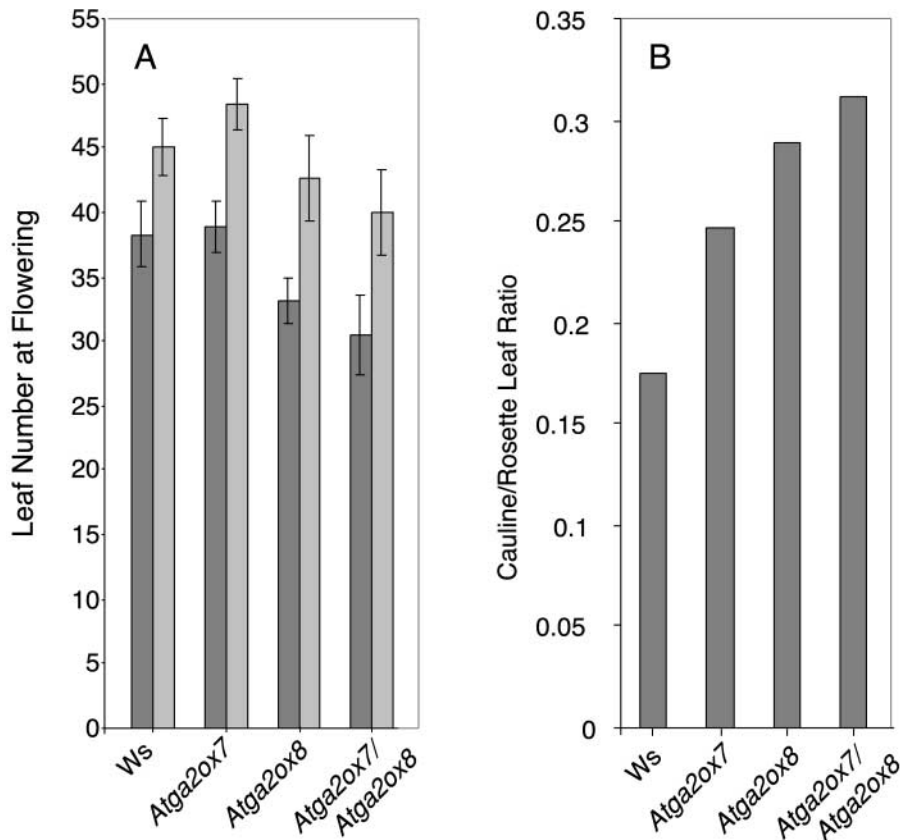


Figure 6. Leaf Numbers of Loss-of-Function Mutants at Flowering.

(A) Primary leaf number at flowering of the loss-of-function mutants *Atga2ox7*, *Atga2ox8*, and the *Atga2ox7 Atga2ox8* double mutant. Dark bars denote rosette leaves, and light bars denote total leaves. Error bars indicate \pm SD. Ws, Wassilewskija.

(B) Ratio of cauline leaves to rosette leaves at flowering.

levels of GA_4 and GA_9 (Table 5). Previous studies have shown that GA application results in feedback inhibition of the GA biosynthetic pathway gene *GA5* (Phillips et al., 1995; Xu et al., 1999). Therefore, we investigated whether *Atga2ox7 Atga2ox8* mutants displayed altered levels of *GA5* mRNA. Indeed, two independent experiments demonstrated that *GA5* expression levels were lower in *Atga2ox7 Atga2ox8* double mutants than in the wild type (Figure 9). Thus, the loss of *AtGA2ox7* and *AtGA2ox8* activity may lead to increased levels of active GAs, which in turn may result in feedback inhibition of the expression of GA biosynthetic genes.

DISCUSSION

This study describes the identification, using an activation-tagging mutant screen (Weigel et al., 2000), of two Arabidopsis loci that cause a dominant dwarf phenotype upon

activation. Increased expression of either of these two loci results in a GA deficiency phenotype that is associated with a reduction in the levels of both GA precursors and active GAs. The genes (*AtGA2ox7* and *AtGA2ox8*) responsible for the dwarf phenotypes exhibit similarity to dioxygenases involved in GA metabolism. However, *AtGA2ox7* and *AtGA2ox8* proteins are more similar to each other than to other genes in the Arabidopsis genome. Thus, *AtGA2ox7* and *AtGA2ox8* form a class within the GA dioxygenase superfamily that represents a novel aspect of GA metabolism.

Studies of the enzymatic activity of *AtGA2ox7* and *AtGA2ox8* demonstrate that these proteins catalyze a novel reaction: both proteins act as 2-oxidases that hydroxylate carbon 2 of C_{20} -GA precursors (e.g., GA_{12}) but not C_{19} -GAs. The 2 β -hydroxylation of C_{20} -GA precursors should render them unable to be converted to active GAs and thus decrease the levels of active GAs and cause a dwarf phenotype. The specificity of these enzymes for C_{20} -GAs but not C_{19} -GAs predicts that plants that are dwarfed by the increased expression of *AtGA2ox7* or *AtGA2ox8* should be

fully GA responsive. Indeed, the dose–response relationship for elongation versus the amount of applied GA is nearly identical in *AtGA2ox8_{ACT}* and the GA biosynthetic mutant *ga1-11*.

Because overexpression of *AtGA2ox7* and *AtGA2ox8* results in decreased levels of active GAs and dwarf phenotypes, it was of interest to determine whether the loss of these genes would cause increased GA levels. Gas chromatography–mass spectrometry analysis of the shoots of mature plants revealed that the double loss-of-function mutant *Atga2ox7 Atga2ox8* contained twofold to fourfold higher levels of GA₄ and GA₉ than the wild type. The *Atga2ox7 Atga2ox8* double mutant and the *Atga2ox8* single mutant also displayed phenotypes typical of plants treated with GAs: flowering in short days after producing fewer rosette leaves but more cauline leaves than the wild type, longer hypocotyls than the wild type, and reduced sensitivity to the inhibition of germination by the GA biosynthesis inhibitor ancymidol, presumably as a result of increased levels of active GAs in the seeds. It is interesting that the *Atga2ox8* single mutant exhibits seedling phenotypes but the *Atga2ox7* single mutant does not. Consistent with this observation, the *Atga2ox8* mRNA but not the *Atga2ox7* mRNA was detectable by RT-PCR in seedlings (data not shown). Although these data indicate that the loss of *AtGA2ox7* and *AtGA2ox8* activity results in phenotypes associated with increased GA levels, these phenotypes are relatively weak compared with, for example, a constitutive GA signaling mutant such as *spindly* (Jacobsen and Olszewski, 1993).

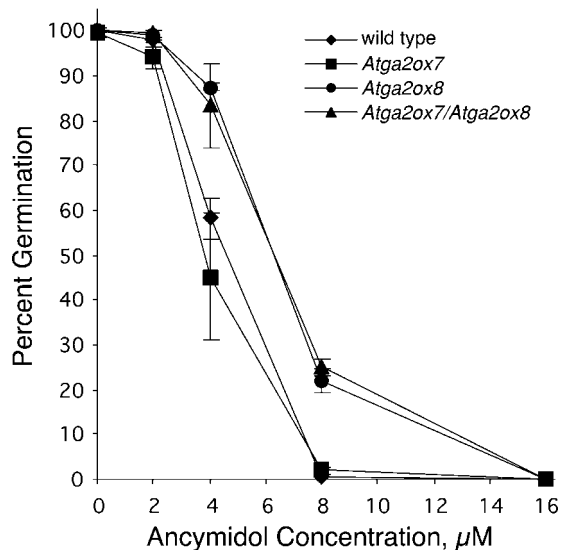


Figure 7. Percentage Germination of Loss-of-Function Mutants Grown on the GA Biosynthesis Inhibitor Ancymidol.

Germination was scored at 11 days after imbibition and incubation at 22°C in continuous light. Error bars indicate \pm SD.

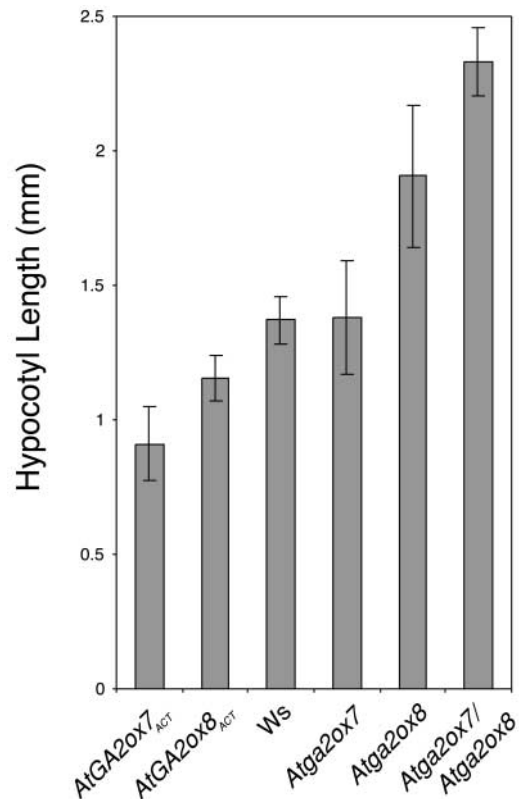


Figure 8. Hypocotyl Length of Loss-of-Function and Activation-Tagged Mutants.

Plants were grown in continuous cool-white fluorescent light ($50 \mu\text{mol}\cdot\text{m}^{-2}\cdot\text{s}^{-1}$). The *AtGA2ox7_{ACT}* and *AtGA2ox8_{ACT}* mutants exhibited shorter hypocotyls than the wild type, whereas loss-of-function *Atga2ox8* and *Atga2ox7 Atga2ox8* double mutants displayed longer hypocotyls than the wild type. Error bars indicate \pm SD. Ws, Wassilewskija.

The relatively weak phenotypes associated with the *Atga2ox7* and *Atga2ox8* single and double loss-of-function mutants might be the result of feedback compensation in the GA biosynthetic pathway. In the *Atga2ox7 Atga2ox8* double mutant, GA₅ mRNA levels were reduced. GA₅ encodes an enzyme involved in GA biosynthesis, and GA₅ expression is subject to feedback regulation (Xu et al., 1999). The reduction in GA₅ expression in the *Atga2ox7 Atga2ox8* double mutant indicates that loss of the activities of these genes is sufficient to affect this feedback system and to reduce GA biosynthetic activity. In the double mutant, the levels of GA₂₄ and GA₅₃ also were lower, indicating that this feedback also might affect earlier steps in the biosynthetic pathway. The lower level of precursors in the double mutant also should contribute to the decreased severity of the double mutant phenotype.

The weak phenotype of the double mutant also could result if *AtGA2ox7* and *AtGA2ox8* are expressed primarily in certain tissues or cell types, at specific stages of development, or in response to specific inductive conditions. Thus, the mutant analyses may not have been performed under the proper conditions to reveal additional phenotypes, and measurements of whole-plant GA levels would not reveal differences in GA levels in specific cell types. The transcripts of *AtGA2ox7* and *AtGA2ox8* were not detectable by RNA gel blot analysis, and only *AtGA2ox8* was detected by RT-PCR in seedling tissue after >38 cycles. *AtGA2ox7* was not detected in any tissue examined, and *AtGA2ox8* was not detected in any adult tissue. Another possible explanation for the weak phenotype of the double mutant could be the existence of additional C₂₀-GA 2-oxidases in the genome. However, the Arabidopsis genome does not contain other genes predicted to encode proteins that have high homology with *AtGA2ox7* or *AtGA2ox8*.

The unique activities of *AtGA2ox7* and *AtGA2ox8* may provide a strategy for the development of new dwarf or semidwarf varieties of crop and ornamental plant species. A major component of the increased yield of the "green revolution" varieties of crop plants is the introduction of dwarfed varieties (Peng et al., 1999; Spielmeier et al., 2002). The creation of such varieties has relied upon natural genetic variation within the crop species. The possibility of introducing *AtGA2ox7* or *AtGA2ox8*, other GA-metabolizing enzymes (Thomas et al., 1999), or *GA-INSENSITIVE* (Fu et al., 2001) to create dominant dwarf varieties without the need to identify mutants or native genes involved in GA metabolism or perception from each plant species should facilitate the production of new crop varieties. *AtGA2ox7* and *AtGA2ox8* may be particularly useful in this regard because the substrates of *AtGA2ox7* and *AtGA2ox8* are common intermediates in the GA biosynthetic pathway of most flowering plants (Hedden and Phillips, 2000); thus, the expression of these genes should cause dwarfing in a wide range of species. Indeed, we have shown that these Arabidopsis genes

Table 5. GA Content of Wild-Type Arabidopsis (Accession Wassilewskija [Ws]) and Mutant Lines

GAs	Ws	<i>Atga2ox7</i>	<i>Atga2ox8</i>	<i>Atga2ox7/Atga2ox8</i>
Non-13-hydroxylated				
GA ₂₄	46.76	44.07	36.85	12.78
GA ₉	1.03	1.10	1.58	3.75
GA ₄	1.42	1.27	1.62	2.93
13-Hydroxylated				
GA ₅₃	7.27	6.28	5.06	2.41
GA ₄₄	0.85	0.97	1.05	2.24
GA ₁₉	11.89	15.45	15.03	17.59
GA ₂₀	0.23	0.16	0.28	0.98
GA ₁	0.37	0.23	0.24	0.43

All values are ng/g dry weight.

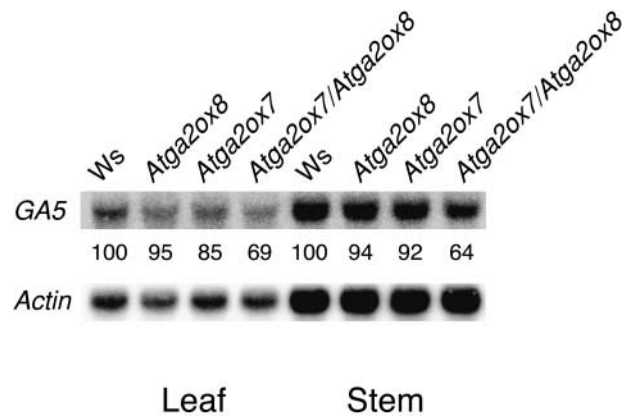


Figure 9. *GA5* (*AtGA2ox1*) mRNA Levels in Loss-of-Function Mutants.

The *GA5* signal was normalized to the *Actin* signal and then compared with the wild type. Relative *GA5* intensities are shown under each lane as the percentage of signal relative to the wild type. Ws, Wassilewskija.

are capable of causing extreme dwarfing in tobacco. Furthermore, because *AtGA2ox7* and *AtGA2ox8* do not modify (or hydroxylate) C₁₉-GAs, active C₁₉-GAs can be applied to *AtGA2ox7*- or *AtGA2ox8*-derived dwarf plants to rescue the dwarf phenotypes. By altering the expression levels and/or spatial expression patterns of *AtGA2ox7* and *AtGA2ox8*, it should be possible to produce plants with a range of dwarf phenotypes.

METHODS

Plant Growth Conditions

Arabidopsis thaliana plants were grown under cool-white fluorescent light (100 $\mu\text{mol}\cdot\text{m}^{-2}\cdot\text{s}^{-1}$; Sylvania, Danvers, MA) at $22 \pm 1^\circ\text{C}$ in Fafard Germination Mix (Fafard Co., Agawam, MA). Plants were fertilized with 2 g/L Dyna-Grow 7-9-5 fertilizer (Dyna-Grow Corp., San Pablo, CA) at 2-week intervals. Daylengths were 8 h of light and 16 h of darkness for short days and 16 h of light and 8 h of darkness for long days. Germination assays were performed on Murashige and Skoog (1962) medium, pH 5.8, that was supplemented with 5.5 g/L agar, 0.5 g/L Mes (Sigma), and 1% Suc. Ancyimidol (Sigma) was added to autoclaved medium from a filter-sterilized $\times 100$ stock solution.

Plants to be used for gibberellin (GA) quantification were grown in trays as described (Talon et al., 1990a). Short-day conditions consisted of 9 h of light (23°C) from fluorescent and incandescent lamps at 150 $\mu\text{mol}\cdot\text{m}^{-2}\cdot\text{s}^{-1}$ and 15 h darkness at 20°C. For long days, the 9-h main light period was extended to 15 h with light from incandescent lamps at 25 $\mu\text{mol}\cdot\text{m}^{-2}\cdot\text{s}^{-1}$. Plants were grown in short days until flower primordia began to appear. At that time, the plants were ex-

posed to 3 or 4 long days before harvest. Plants with stems, if present, were harvested and frozen in liquid N₂. All plant material was lyophilized.

Isolation of *AtGA2ox7* and *AtGA2ox8* Knockout Alleles

The BASTA T-DNA (accession Wassilewskija) population of the Wisconsin T-DNA collection was screened for insertion (i.e., knockout) alleles of *AtGA2ox7* and *AtGA2ox8* at the Arabidopsis Knockout Facility (<http://www.biotech.wisc.edu/Arabidopsis/default.htm>) according to Krysan et al. (1999). Gene-specific primers for *AtGA2ox7* (5'-CTAACTAGTGGTGAGGAGGTCAAAC-3' and 5'-TCGAGATAAGGACATACGAAGAAAG-3') and *AtGA2ox8* (5'-TGTGTCTCTCCTCAC-AACACG-3' and 5'-AGGAACCTAGGAAGGCCAAC-3') were used in combination with the left border T-DNA primer JL202 (Krysan et al., 1999) to identify knockout mutants. *AtGA2ox7* is in BAC F8A12.18, and *AtGA2ox8* is in BAC F7J7.140.

Identification of DNA Flanking the Site of T-DNA Insertion

Identification of the T-DNA insertion site in the *AtGA2ox7_{ACT}* and *AtGA2ox8_{ACT}* lines in Arabidopsis was determined by thermal asymmetrical intercalated (TAIL)-PCR. Genomic DNA for use in TAIL-PCR was prepared as described (Liu et al., 1995). PCR reactions were conducted using hot-start addition of Takara ExTaq enzyme (Panvera, Madison, WI). Two rounds of PCR amplifications were used to isolate DNA flanking the T-DNA insertion site. Fifteen picomoles of the left border T-DNA primer JL202 was used with 150 pmol of the partially degenerate primer AD-2 (5'-NGTCGASWGANAWGAA-3') for the first PCR reaction. Conditions for the first reaction were as follows: (1) 96°C for 5 min; (2) 94°C for 10 s; (3) 65°C for 30 s; (4) 72°C for 1 min; (5) repeat four additional cycles of steps 2 through 4; (6) 94°C for 10 s; (7) 25°C for 3 min; (8) ramp to 72°C over 3 min; (9) 72°C for 3 min; (10) 94°C for 10 s; (11) 65°C for 30 s; (12) 72°C for 1 min; (13) repeat one additional cycle of steps 10 through 13; (14) 94°C for 10 s; (15) 44°C for 1 min; (16) 72°C for 1 min; (17) repeat 14 additional cycles of steps 10 through 16; (18) 72°C for 3 min; and (19) 4°C until needed.

DNA produced in the first PCR was diluted 1:50, and 1 μL of this dilution was used for the second round of PCR. Similar to the first reaction, 15 pmol of the left border primer was used with 15 pmol of AD-2 for amplification. The PCR cycle conditions were as follows: (1) 96°C for 5 min; (2) 94°C for 10 s; (3) 61°C for 30 s; (4) 72°C for 1 min; (5) repeat one additional cycle of steps 2 through 4; (6) 94°C for 10 s; (7) 44°C for 1 min; (8) 72°C for 1 min; (9) repeat 17 additional cycles of steps 2 through 8; (10) 72°C for 4 min; and (11) 4°C until needed. The resulting PCR products were sequenced with the JL270 primer.

Generation of Overexpression Constructs of *AtGA2ox7* and *AtGA2ox8*

The overexpression constructs of *AtGA2ox7* and *AtGA2ox8* were created by PCR amplification of genomic DNA from the start to the stop codon of the putative open reading frame of the dioxygenases. The primers used to generate overexpression of *AtGA2ox8* were 5'-AAAGGATCCATGGACCCACCATTC AACGAAATATAC-3' and 5'-AAAGAGCTCTTAAGGAACCTAGGAAGGCCAAC-3' (restriction sites are shown in boldface, and the sequence corresponding to *AtGA2ox8* is underlined), which generated a 3838-bp fragment that was digested with BamHI and SacI and ligated into the BamHI and

SacI sites of pRAM1. pRAM1 was created by ligating the HindIII-EcoRI fragment of pBI121 containing the 35S promoter and nopaline synthase terminator sequences into the HindIII and EcoRI sites of pPZP211 (Harberd et al., 1998). The same *AtGA2ox8* primer pair produced a 1017-bp cDNA fragment from a cDNA preparation (see below) that was used to create a cDNA overexpression construct in pRAM1. Similarly, *AtGA2ox7* genomic and cDNA overexpression constructs were produced with the primer pair 5'-AAAGGATCC-ATGGCTTCTCAACCTCCCTT-3' and 5'-AAAGAGCTCTCAATGAG-AAACCTGGACAAG-3', which produced 2171-bp genomic and 1011-bp cDNA fragments. These were cloned into pRAM1 as described above. The constructs were transferred into *Agrobacterium tumefaciens* strain ABI and transformed into Arabidopsis by the floral dip method (Clough and Bent, 1998).

mRNA Detection by Reverse Transcriptase-Mediated PCR

RNA was prepared from tissue that had been immediately frozen in liquid N₂. RNA was isolated with TRI reagent (Sigma) according to instructions for subsequent reverse transcription reactions. Five micrograms of total RNA was annealed to 500 ng of random decamer oligonucleotides (Integrated DNA Technologies, Coralville, IA). Superscript II reverse transcriptase (Gibco Life Technologies, Gaithersburg, MD) was used to generate cDNA. Takara ExTaq was used for PCR amplification of cDNA. PCR conditions were 26 cycles of 95°C for 15 s, 55°C for 30 s, and 72°C for 2 min.

Production of *AtGA2ox7* and *AtGA2ox8* Proteins

AtGA2ox7 and *AtGA2ox8* cDNAs were obtained by reverse transcription-based PCR as described above. Primers were designed to allow simple cloning of the cDNAs into pET-28a (Promega, Madison, WI). The *AtGA2ox8* cDNA was amplified with 5'-AAAGGATCCATGGACCCACCATTC AACGAAATATAC-3' and 5'-AAAGAGCTCAGG-AAACCTAGGAAGGCCAAC-3' and subsequently ligated into pET-28a in the BamHI and SacI sites of the polylinker. The *AtGA2ox7* cDNA was amplified with 5'-AAAGGATCCATGGCTTCTCAACCTCCCTT-3' and 5'-AAAGAGCTCAATGAGAAACCTGGACAAG-3' and also cloned into pET-28a using the BamHI and SacI restriction sites.

The full-length cDNA clones pET-*AtGA2ox7* and pET-*AtGA2ox8* were transformed into *Escherichia coli* strain BL21pLysS. A starter culture (25 mL) was added to 0.5 L of Luria-Bertani medium containing 100 mg/L kanamycin and incubated at 37°C with vigorous shaking. When the OD₆₀₀ had reached 0.6, isopropylthio-β-galactoside was added to a final concentration of 3 mM and the culture was incubated for another 2 h at 30°C. The cells were harvested and suspended in lysis buffer (100 mM Tris-HCl, pH 7.5, and 10 mg/mL lysozyme) and shaken at room temperature for 10 min. After brief sonication, the suspension was frozen in liquid N₂ and then thawed in an ice bath for 15 min. The lysates were centrifuged at 13,000 rpm for 20 min, and the supernatant was stored at -80°C until use for enzyme assays.

RNA Gel Blot Analysis

Total RNA was isolated from leaves and stems using the TRIzol reagent (Invitrogen, Carlsbad, CA). Forty micrograms of total RNA was fractionated on a 1.2% agarose gel in the presence of formaldehyde (Sambrook et al., 1989), transferred to nitrocellulose, and probed

with ^{32}P -dCTP-labeled cDNA using the Random Primers DNA Labeling System (Gibco BRL). Hybridization was performed at 42°C using a 50% formamide system (Sambrook et al., 1989). Membranes were washed twice for 10 min in $2 \times \text{SSC}$ ($1 \times \text{SSC}$ is 0.15 M NaCl and 0.015 M sodium citrate) at room temperature and then twice for 10 min in $0.2 \times \text{SSC}$ with 0.1% SDS at 65°C (high stringency). At low stringency, the membrane was washed once for 10 min in $2 \times \text{SSC}$ at room temperature and then washed again for 10 min in $2 \times \text{SSC}$ at 63°C. The relative amounts of mRNA were determined with a PhosphorImager (Molecular Dynamics, Sunnyvale, CA). Each experiment was repeated at least twice with similar results.

Enzyme Assays and Product Analysis

Enzyme assays with recombinant proteins were performed with ~30,000 dpm of ^{14}C -labeled GAs. The reaction mixture consisted of 80 μL of enzyme, 10 μL of 100 mM Tris-HCl, pH 7.5, and 10 μL of cofactors to give a final concentration of 5 mM ascorbate, 5 mM 2-oxoglutarate, and 0.5 mM FeSO_4 . Cofactors were replenished after 1 h. The mixture was incubated for up to 6 h with gentle shaking. The products were separated by reverse-phase HPLC with online radioactivity detection (Zeevaert et al., 1993). For product identification by gas chromatography-mass spectrometry (see below), larger scale enzyme assays were used.

Gibberellin Extraction and Quantification

The procedures for extraction, purification, and quantification of endogenous GAs with deuterated GAs as internal standards were as described (Talon et al., 1990a; Zeevaert et al., 1993), except that the charcoal column step was omitted. The gas chromatograph was equipped with a DB-5MS capillary column (30 m \times 0.32 mm \times 0.25 μm film; J&W Scientific, Folsom, CA), which was operated in splitless mode. The oven temperature was kept at 100°C for 1 min after sample injection and then programmed from 100 to 230°C at 40°C/min, from 230 to 280°C at 8°C/min, and finally to 300°C at 20°C/min.

Upon request, all novel materials described in this article will be made available in a timely manner for noncommercial research purposes.

Accession Numbers

The accession numbers for the genes mentioned in this article are as follows: AC079284 and AL021960 (*AtGA2ox7* and *AtGA2ox8*); AJ132435, AJ132436, and AJ132437 (*AtGA2ox1* to *AtGA2ox3*); X83379, X83380, and X83381 (*AtGA2ox1* to *AtGA2ox3*); and L37126 and T51691 (*AtGA3ox1* and *AtGA3ox2*).

ACKNOWLEDGMENTS

We thank Maarten Koornneef for providing seeds of the *ga1-11* mutant in Wassilewskija background. We thank Detlef Weigel for supplying the pSKI015 vector. This work was supported by the College

of Agricultural and Life Sciences and the Graduate School of the University of Wisconsin and by grants to R.M.A. from the Consortium for Plant Biotechnology Research and the National Science Foundation and by the U.S. Department of Agriculture (Grant 97-35304-4692) and the U.S. Department of Energy (Grant DE-FG02-91ER20021 to J.A.D.Z.).

Received July 8, 2002; accepted October 21, 2002.

REFERENCES

- Chiang, H.H., Hwang, I., and Goodman, H.M. (1995). Isolation of the *Arabidopsis GA4* locus. *Plant Cell* **7**, 195–201.
- Clough, S.J., and Bent, A.F. (1998). Floral dip: A simplified method for *Agrobacterium*-mediated transformation of *Arabidopsis thaliana*. *Plant J.* **16**, 735–743.
- Fu, X., Sudhakar, D., Peng, J., Richards, D.E., Christou, P., and Harberd, N.P. (2001). Expression of *Arabidopsis GAI* in transgenic rice represses multiple gibberellin responses. *Plant Cell* **13**, 1791–1802.
- Harberd, N.P., King, K.E., Carol, P., Cowling, R.J., Peng, J., and Richards, D.E. (1998). Gibberellin: Inhibitor of an inhibitor of...? *Bioessays* **20**, 1001–1008.
- Hedden, P., and Phillips, A.L. (2000). Gibberellin metabolism: New insights revealed by the genes. *Trends Plant Sci.* **5**, 523–530.
- Helliwell, C.A., Chandler, P.M., Poole, A., Dennis, E.S., and Peacock, W.J. (2001). The CYP88A cytochrome P450, *ent*-kaurenoic acid oxidase, catalyzes three steps of the gibberellin biosynthesis pathway. *Proc. Natl. Acad. Sci. USA* **98**, 2065–2070.
- Helliwell, C.A., Sheldon, C.C., Olive, M.R., Walker, A.R., Zeevaert, J.A., Peacock, W.J., and Dennis, E.S. (1998). Cloning of the *Arabidopsis ent*-kaurene oxidase gene *GA3*. *Proc. Natl. Acad. Sci. USA* **95**, 9019–9024.
- Jacobsen, S.E., and Olszewski, N.E. (1993). Mutations at the *SPINDLY* locus of *Arabidopsis* alter gibberellin signal transduction. *Plant Cell* **5**, 887–896.
- Koornneef, M., and van der Veen, J.H. (1980). Induction and analysis of gibberellin sensitive mutants. *Theor. Appl. Genet.* **58**, 257–263.
- Krysan, P.J., Young, J.C., and Sussman, M.R. (1999). T-DNA as an insertional mutagen in *Arabidopsis*. *Plant Cell* **11**, 2283–2290.
- Liu, Y.G., Mitsukawa, N., Oosumi, T., and Whittier, R.F. (1995). Efficient isolation and mapping of *Arabidopsis thaliana* T-DNA insert junctions by thermal asymmetric interlaced PCR. *Plant J.* **8**, 457–463.
- Martin, D.N., Proebsting, W.M., and Hedden, P. (1999). The *SLENDER* gene of pea encodes a gibberellin 2-oxidase. *Plant Physiol.* **121**, 775–781.
- Murashige, T., and Skoog, F. (1962). A revised medium for rapid growth and bioassays with tobacco tissue culture. *Physiol. Plant.* **15**, 473–497.
- Olszewski, N., Sun, T.P., and Gubler, F. (2002). Gibberellin signaling: Biosynthesis, catabolism, and response pathways. *Plant Cell* **14** (suppl.), S61–S80.
- Peng, J., et al. (1999). 'Green revolution' genes encode mutant gibberellin response modulators. *Nature* **400**, 256–261.
- Phillips, A.L., Ward, D.A., Uknes, S., Appleford, N.E., Lange, T., Huttly, A.K., Gaskin, P., Graebe, J.E., and Hedden, P. (1995).

- Isolation and expression of three gibberellin 20-oxidase cDNA clones from *Arabidopsis*. *Plant Physiol.* **108**, 1049–1057.
- Sakamoto, T., Kobayashi, M., Itoh, H., Tagiri, A., Kayano, T., Tanaka, H., Iwahori, S., and Matsuoka, M.** (2001). Expression of a gibberellin 2-oxidase gene around the shoot apex is related to phase transition in rice. *Plant Physiol.* **125**, 1508–1516.
- Sambrook, J., Fritsch, E., and Maniatis, T.** (1989). *Molecular Cloning: A Laboratory Manual*. (Cold Spring Harbor, NY: Cold Spring Harbor Laboratory Press).
- Soltis, P.S., Soltis, D.E., and Chase, M.W.** (1999). Angiosperm phylogeny inferred from multiple genes as a tool for comparative biology. *Nature* **402**, 402–404.
- Spielmeyer, W., Ellis, M.H., and Chandler, P.M.** (2002). Semidwarf (*sd-1*), “green revolution” rice, contains a defective gibberellin 20-oxidase gene. *Proc. Natl. Acad. Sci. USA* **99**, 9043–9048.
- Sun, T.P., and Kamiya, Y.** (1994). The *Arabidopsis* *GA1* locus encodes the cyclase *ent*-kaurene synthetase A of gibberellin biosynthesis. *Plant Cell* **6**, 1509–1518.
- Talon, M., Koornneef, M., and Zeevaart, J.A.D.** (1990a). Endogenous gibberellins in *Arabidopsis thaliana* and possible steps blocked in the biosynthetic pathways of the semidwarf *ga4* and *ga5* mutants. *Proc. Natl. Acad. Sci. USA* **87**, 7983–7987.
- Talon, M., Koornneef, M., and Zeevaart, J.A.D.** (1990b). Accumulation of C₁₉-gibberellins in the gibberellin-insensitive dwarf *gai* of *Arabidopsis thaliana* (L.) Heynh. *Planta* **182**, 501–505.
- Talon, M., and Zeevaart, J.A.D.** (1992). Stem elongation and changes in the levels of gibberellins in shoot tips induced by differential photoperiodic treatments in the long-day plant *Silene armeria*. *Planta* **188**, 457–461.
- Thomas, S.G., Phillips, A.L., and Hedden, P.** (1999). Molecular cloning and functional expression of gibberellin 2-oxidases, multifunctional enzymes involved in gibberellin deactivation. *Proc. Natl. Acad. Sci. USA* **96**, 4698–4703.
- Weigel, D., et al.** (2000). Activation tagging in *Arabidopsis*. *Plant Physiol.* **122**, 1003–1013.
- Wilson, R.N., Heckman, J.W., and Somerville, C.R.** (1992). Gibberellin is required for flowering in *Arabidopsis thaliana* under short days. *Plant Physiol.* **100**, 403–408.
- Xu, Y.L., Li, L., Gage, D.A., and Zeevaart, J.A.D.** (1999). Feedback regulation of *GA5* expression and metabolic engineering of gibberellin levels in *Arabidopsis*. *Plant Cell* **11**, 927–936.
- Zeevaart, J.A.D., Gage, D.A., and Talon, M.** (1993). Gibberellin A₁ is required for stem elongation in spinach. *Proc. Natl. Acad. Sci. USA* **90**, 7401–7405.